

# Non-resonant electric quantum control of individual on-surface spins

S. A. Rodríguez<sup>1</sup>, S. S. Gómez<sup>1</sup>, J. Fernández-Rossier<sup>2</sup> <sup>\*</sup>, A. Ferrón<sup>1</sup>

(1) *Instituto de Modelado e Innovación Tecnológica (CONICET-UNNE) and Facultad de Ciencias Exactas, Naturales y Agrimensura, Universidad Nacional del Nordeste,*

*Avenida Libertad 5400, W3404AAS Corrientes, Argentina.*

(2) *International Iberian Nanotechnology Laboratory (INL),*

*Av. Mestre José Veiga, 4715-330 Braga, Portugal.*

(Dated: May 16, 2024)

Quantum control techniques play an important role in manipulating and harnessing the properties of different quantum systems, including isolated atoms. Here, we propose to achieve quantum control over a single on-surface atomic spin using Landau-Zener-Stückelberg-Majorana (LZSM) interferometry implemented with Scanning Tunneling Microscopy (STM). Specifically, we model how the application of time-dependent, non-resonant AC electric fields across the STM tip-surface gap makes it possible to achieve precise quantum state manipulation in an isolated Fe atom on a MgO/Ag(100) surface. We propose a protocol to combine Landau Zener tunneling with LZSM interferometry that permits one to measure the quantum spin tunneling of an individual Fe atom. The proposed experiments can be implemented with ESR-STM instrumentation, opening a new venue in the research of on-surface single spin control.

PACS numbers:

The control of two-level quantum systems plays a central role in developing quantum technologies, such as quantum sensing and quantum computing. Two complementary strategies can be used to achieve this goal. First, resonant excitation with either continuous wave perturbations or pulses<sup>1–4</sup>. Second, parametric manipulation of systems in the neighborhood of avoided crossings, that cause non-adiabatic transitions, which, together with quantum interference, lead to controllable state transitions<sup>5,6</sup>. The protocol discussed is commonly known as Landau-Zener-Stückelberg-Majorana (LZSM) interference<sup>5,6</sup>, and experiments in various systems have demonstrated its successful implementation. Notable examples include superconducting qubits<sup>7–10</sup>, molecular nanomagnets<sup>11,12</sup>, semiconductor artificial atoms<sup>13</sup>, impurity-based qubits<sup>14</sup>, and NV centers<sup>15</sup>, among several others. In addition, LZSM interferometry has been extensively used for spectroscopy in different systems, including Josephson flux qubits<sup>7,16</sup>. Is worth mentioning that Landau Zener (LZ) transitions have previously been employed to measure very small tunnel splittings in single-molecule magnets<sup>11</sup> and to demonstrate quantum state control in Ho, where the hyperfine interaction creates several avoided level crossings<sup>17</sup>.

This work aims to lay the theoretical foundations of LZSM interferometry for individual surface spin controlled *electrically* with a Scanning Tunneling Microscope (STM). Our proposal requires instrumentation identical to state-of-the-art STM electron spin-resonance (STM-ESR) experiments<sup>18,19</sup>. There, the spin of the surface is driven, electrically<sup>19,20</sup>, by a radio frequency voltage with frequency  $f$ . So far, it has been used to perform both

continuous-wave experiments and dynamical control with voltage pulses, with the frequency  $f$  close to the resonance frequency  $f_0$ . The manipulation of the quantum state of an individual spin has been demonstrated<sup>21–23</sup>. In our proposal, the driving frequency is far from resonance, and the driving mechanisms are thus different from previous works<sup>19,21,23–31</sup> in ESR-STM.

It is widely accepted<sup>19,20,32</sup> that the surface spin is coupled to the RF electric field associated with the RF voltage drop at the STM-surface junction. Piezoelectric displacement of the surface spin<sup>20,29,33</sup> together with distance-dependent spin interactions between the surface spin and the magnetic tip provides a natural route for the coupling of the spin to the electric field. Here, we propose to leverage this piezoelectric coupling to carry out LZSM manipulation. We illustrate the application of our theory to the case of Fe on MgO, the physical system first studied with STM-ESR<sup>19</sup> and depicted in Fig 1(a). On this surface, Fe is a non-Kramers doublet with  $S = 2$ , and it is expected<sup>20,34,35</sup> to feature quantum spin tunneling splitting  $\Delta$ , between two states with  $S_z = \pm 2$ , providing thereby a natural scenario for the existence of an avoided crossing, essential for employing LZSM interference to implement quantum control. We note however that the analysis will apply to a wide class of non-Kramers doublets<sup>36</sup>, including atomic and molecular surface-spins.

The starting point of our analysis is the description of the ground state doublet of Fe on MgO in terms of a two-level system (TLS):

$$H_{TLS}(t) = -24\mathcal{F}(t)\hat{\sigma}_x - h_{\text{eff}}(t)\hat{\sigma}_z \quad (1)$$

where  $\hat{\sigma}_{x,z}$  are Pauli matrices acting on the subspace  $S = 2, S_z = \pm 2$  that expands the ground state doublet of Fe on MgO, for which ESR-STM was first demonstrated<sup>19</sup> and has been studied in detail before<sup>19,20,34,35</sup>. This model features the competition between quantum spin

<sup>\*</sup>On leave from Departamento de Física Aplicada, Universidad de Alicante, 03690 Spain

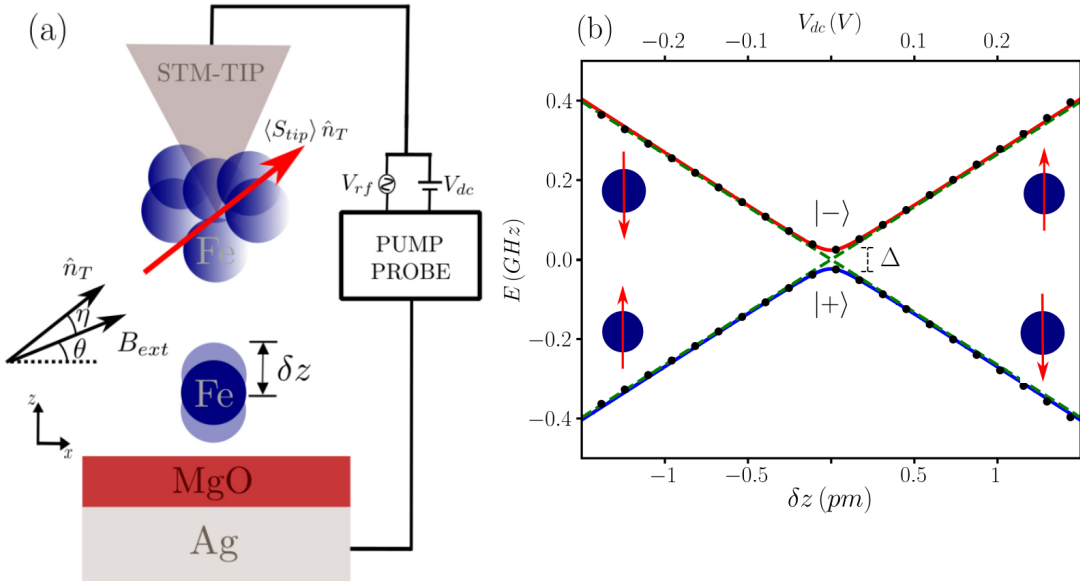


FIG. 1: (a) Sketch of the experimental setup: a spin-polarized STM drives the spin of a single Fe atom on a MgO surface on top of silver. The external magnetic field forms an angle  $\theta$  with the surface. Additionally, we can observe that the magnetization of the tip does not align with this field due to its anisotropy, forming an angle  $\eta$  with the external field. (b) Lowest energy levels of Fe as a function of the piezoelectric displacement or  $V_{dc}$ , as calculated with Hamiltonians Eq. (1) (dots) and Eq. (3) (continuous lines).

tunneling term  $\mathcal{F}$ , driven by the interplay of crystal field and spin-orbit coupling, and the coupling of the Fe electronic spin to an effective magnetic field given by the sum of three contributions<sup>26,31,35</sup>: external magnetic field, stray-field of the magnetic atoms in the tip and exchange interaction with these atoms, treated semiclassically (see also supplementary material (SM) for more detail). Importantly, Eq. (1) describes as well the low energy spectrum of a large variety of integer spin non-Kramers doublets.

We now make the key observation that it is possible to use the STM tip to control both energy scales,  $\mathcal{F}$  and  $h_{eff}$ . The voltage across the tip-sample junction has a constant component,  $V_{dc}$ , and an oscillating component,  $V_{rf}(t)$ , that lead to a piezoelectric distortion of the surface atom<sup>20,35,37</sup>:

$$\delta z(t) \simeq \frac{q}{kd_{tip}} (V_{dc} + V_{rf}(t)), \quad (2)$$

and this displacement modifies the crystal field<sup>19</sup>, and hence  $\mathcal{F}$ , as well as the  $g$  factor<sup>37</sup> and the magnitude of the dipolar and exchange coupling with the tip, that have an impact on  $h_{eff}$ <sup>35</sup>. Our microscopic analysis<sup>20,35,37</sup>, based on a multiplet Hamiltonian (see SM for details), gives us an estimate of how these quantities depend on the voltage. Given the smallness of the displacements, we can Taylor expand the Hamiltonian keeping only the terms linear in  $\delta z$ . In this limit we can write  $\mathcal{F} = \mathcal{F}_{eq} + \alpha_{\mathcal{F}} \delta z$  and  $h_{eff} = h_{eff}^{eq} + \alpha_h \delta z$  (see SM). We locate the STM-tip at the tip-adatom distance,  $z_n$ , that minimizes the tip-induced effective magnetic field on the

surface spin (NOTIN point)<sup>31,35</sup>, we set  $B_{ext} = 0$  and we use that  $\alpha_h \simeq 270\text{GHz/nm} \gg 24|\alpha_{\mathcal{F}}| \simeq 1\text{GHz/nm}$ , so that it is safe to ignore the modulation of the first term. As a result, we can write Hamiltonian Eq. (1) as:

$$H_{TLS}^s(t) = -\frac{\Delta}{2} \hat{\sigma}_x - \frac{\varepsilon(t)}{2} \hat{\sigma}_z \quad (3)$$

The first energy scale,  $\Delta = 48\mathcal{F}_{eq}$ , controlled by the quantum spin tunneling of the Fe atom, is known as<sup>5,6</sup> tunneling amplitude. For zero bias, our calculation yields  $\Delta \simeq 0.05\text{GHz}$ .<sup>35</sup> The second term in Eq. (3) is known as the energy bias  $\varepsilon(t) = 2\alpha_h \delta z(t)$ . It is customary<sup>5,6</sup> to refer to the eigenstates of Hamiltonian Eq. (3) with  $\Delta = 0$  as the diabatic states. In this system, they correspond to the eigenstates of  $S_z = \pm 2$ . The adiabatic eigenvalues consist of the instantaneous eigenstates of the time-dependent Hamiltonian Eq. (3)<sup>5,6</sup>, where both  $\Delta$  and  $\varepsilon$  are finite.

The two energy levels calculated diagonalizing the system Hamiltonian as a function of  $\delta z$  or  $V_{dc}$  are depicted in Fig. 1(b). Black dots show the adiabatic eigenvalues for the Hamiltonian Eq. (1) and continuous lines were obtained for the simplified version Eq. (3). For small displacements (small voltages) calculations performed with the simplified version Eq. (3) agree with the exact solution obtained using Eq. (1). For larger values of voltage (bigger displacement of the atom) we observe some tiny differences between both solutions.

We now illustrate how the spin orientation of the Fe adatom can be controlled with pulses of AC voltages de-

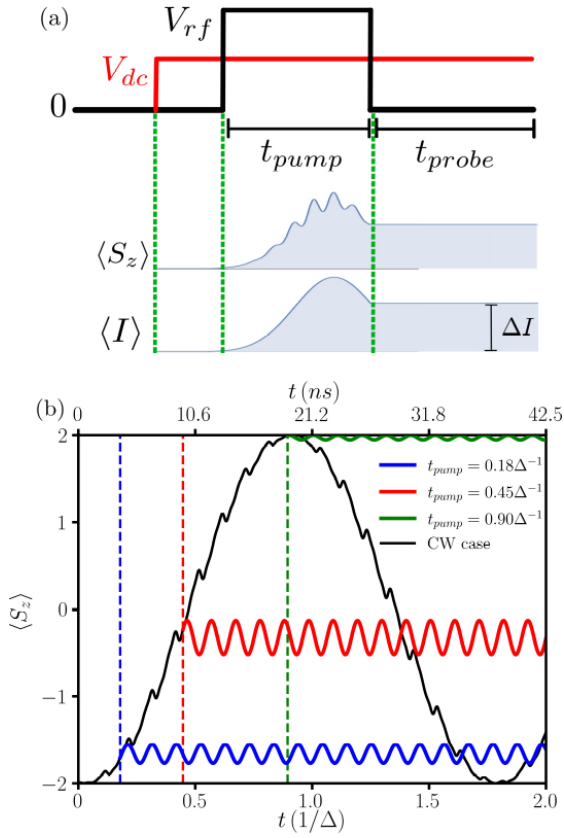


FIG. 2: (a) Sketch of the time dependence of voltage, Fe magnetization and current. Current flows in response to both DC and AC voltage. After AC voltage train changes the Fe magnetization, and, because of the tunnel magnetoresistance, changes of DC current, making it possible to track the surface spin manipulation. (b) Calculated time evolution of the average surface spin,  $\langle S_z \rangle$ , driven by the STM voltage (both DC and AC) in two different situations: cw-coherent driving (black lines) and pulsed-driving (color lines), for which AC driving is turned-off after an operation time  $t_{pump}$ . Fe magnetization oscillations when pump is off relate to the free evolution in a superposition state. Calculations were performed for  $f = 10\Delta$ ,  $V_{dc} = 200$  mV,  $V_{rf} = 460$  mV and  $B_{ext} = 0$ .

scribed with

$$V_{dc} + V_{rf} \sin \omega t, \quad (4)$$

where  $f = 2\pi\omega$  is the driving frequency, and  $V_{rf}$  is the amplitude. The tip-atom distance is tuned as to be in the NOTIN point, where the tip magnetic field vanishes at the surface spin, leading to  $\varepsilon = 0$  in Eq. (3) when  $V_{dc} = V_{rf} = 0$  and  $B_{ext} = 0$ . The three parameters that can be controlled experimentally are the amplitudes of the DC and RF voltages,  $V_{dc}$ ,  $V_{rf}$ , and the frequency  $f$ . Numerical integration of the Schrödinger equation for Hamiltonian Eq. (1) yields the wave function that permits us to calculate the average off-plane magnetization of the Fe atom,  $\langle S_z \rangle$ . Our numerical simulations (see Fig. 2) show  $\langle S_z \rangle$  as a function of time for fixed values of the frequency,  $V_{dc}$  and  $V_{rf}$  for four cases: continuous wave

(CW) excitation, i.e., with  $V_{rf}$  time-independent (black line), and AC pulses, where  $V_{rf}$  is only finite during a finite interval of time with three different durations. In all cases, we have  $f = 10\Delta$ , that is, completely out of resonance but within the limits of the current state of the art<sup>19</sup>. We find that, as long as the external voltage is on, the spin orientation is being controlled, in a time scale of 20 ns, determined by  $\Delta$ . Fig. 2(b) illustrates the main point of this work: control over pulse duration permits to set the magnetization value at any arbitrary value<sup>38</sup>. The suggested experimental protocol, depicted in Fig. 2(a), should start by turning on  $V_{dc}$  to initialize the system in a state where  $S_z$  is close to either +2 or -2. The DC current measured before the RF pulse acts as a reference. Application the RF voltage pulse of duration  $t_{pump}$  changes the surface spin magnetization state, resulting in a different DC current once the AC pulse is over, on account of tunnel magnetoresistance<sup>19</sup>.

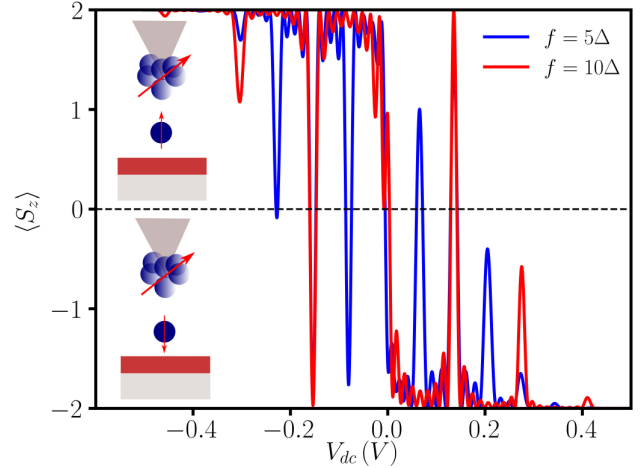


FIG. 3:  $\langle S_z \rangle$  for different operation frequencies  $f$  as a function of the detuning  $V_{dc}$  for  $V_{rf} = 200$  mV,  $t_{pump} = 0.9\Delta^{-1}$  and  $B_{ext} = 0$ .

To rationalize our results, we first discuss some limiting cases and review key concepts. We start analyzing a linear time-dependent perturbation  $V(t) = v_s t$  where the velocity  $v_s = \frac{dV}{dt}$  is the constant that controls the pace of the driving and induces, at the avoided crossing, the so-called Landau-Zener (LZ) transition. LZ transitions from the adiabatic ground state to the excited state occur with probability<sup>5</sup>

$$P_{LZ} = \exp(-2\pi\delta_l) = \exp -\pi \left( \frac{\Delta}{\sqrt{2\hbar \frac{d\varepsilon}{dt}}} \right)^2 \quad (5)$$

where  $\frac{d\varepsilon}{dt} = \alpha_h q v_s / (z_n k)$ . This equation implies an exponential suppression of the transitions out of the adiabatic ground state as  $v_s$  gets smaller, in agreement with the adiabatic theorem.

We now review the harmonic drive case Eq. (4). Here, there is no general analytical solution, to the best of

our knowledge. The dynamics can be approximated<sup>5,6</sup> by adiabatic evolutions of the basis states far from the avoided crossing mediated by nonadiabatic Landau Zener transitions at the avoided crossing (Adiabatic-Impulse Model<sup>5,6</sup>). In this case, the LZ transition probability, at a single passage, is given by the same Eq. (5) with a modified expression for  $\frac{d\varepsilon}{dt} = \alpha_h q v_{rf} / (z_n k)$  where  $v_{rf} = V_{rf} \omega$  is the sweep velocity at the avoided crossing. In the periodic driving case, explicit expressions for the occupation probability have been obtained in the fast or slow driving regime<sup>5,6,16</sup>. Here we will consider the case of fast driving ( $d\varepsilon/dt \gg \Delta^2$ ) and we are going to evaluate the transition probabilities.

For  $V_{dc} > 0$  our system is started in the ground state, which has a spin projection  $S_z = -2$ . We are interested in the probability of exciting transitions in the diabatic basis, i.e., the basis where Fe atom has  $S_z = \pm 2$ . Assuming that at  $t = 0$  the system is in the  $S_z = -2$  state, the probability that the system switches to  $S_z = +2$ , in the fast-driving regime is approximately given as<sup>5,6</sup>

$$P_{-2 \rightarrow +2}(t) = \sum_n \frac{\Gamma_n^2}{2\Omega_n^2} (1 - \cos(\Omega_n t))$$

$$\Omega_n = \sqrt{(n\omega - \gamma V_{dc})^2 + \Gamma_n^2} \quad (6)$$

where  $\gamma = 4\pi q \alpha_h / (k z_n)$ ,  $\Gamma_n = \Delta J_n(\gamma V_{rf} / \omega)$  and  $J_n$  is the Bessel function of the first kind.

One way to understand this equation is as follows: for every period of the RF frequency, the wave function undergoes a beam-splitter type of process, where it can either stay in the ground state or be excited. As this beam-splitter process is repeated many times, given the oscillating nature of the driving potential, the final outcome requires the coherent sum of many passages, resulting in an interference pattern.

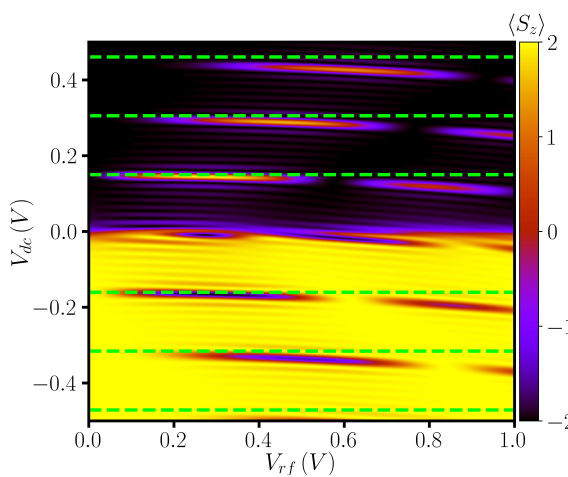


FIG. 4: Contour map of  $\langle S_z \rangle$  as a function of the detuning  $V_{dc}$  and the driving amplitude  $V_{rf}$  for  $t_{pump} = 0.9\Delta^{-1}$  and  $f = 10\Delta$ .

We now discuss our systematic exploration of how dif-

ferent parameters that can be changed in an experiment can be used to optimize the control over the spin state and to explore its physical properties. In Fig. 3 we show the  $V_{dc}$  dependence of the magnetization, measured right at the end of a pulse of fixed duration ( $t_{pump} = 0.9\Delta^{-1}$ ), for two different frequencies. From Eq. (6) it is apparent that the probability of transitions in the diabatic basis is a sum of periodic functions whose amplitude is maximal whenever  $n\omega = \gamma V_{dc}$ , giving a resonance pattern, as obtained in our numerical simulations using Eq. (1). Notably, there are two values of  $V_{dc}$  ( $V_{dc} \simeq \pm 0.18V$ ) for which the spin flipping is complete. Since our model neglects spin relaxation and decoherence, the validity of our predictions will hold as long as the operation time is significantly smaller than  $T_2$ .

We now address the influence of the amplitude of the driving AC voltage,  $V_{rf}$  on the LZSM spin control process. From Eq. (6) we see that  $V_{rf}$  enters  $\Gamma_n$  that controls the amplitude of the different harmonics. Thus, for certain values of  $V_{rf}$  the Bessel functions, and therefore the amplitudes, vanish. This is seen in the phase diagram of Fig. 4, where we plot a contour map for the spin projection of the adatom as a function of the  $V_{dc}$  and  $V_{rf}$ , measured at  $t = t_{pump} = 0.9\Delta^{-1}$ , with a fixed driving frequency  $f = 10\Delta$ . We also plot the position of the resonances obtained using Eq. (6) as horizontal green dashed lines. Here, we can appreciate interference patterns that exhibit fringes that rise from the constructive interference between successive Landau-Zener transitions. The agreement between our numerics and Eq. (6) is very good for the first resonances. The horizontal modulation of the amplitude of the resonances reflects the  $V_{rf}$  dependence of  $\Gamma_n$  anticipated in eq (6). We also note that, in contrast with eq. (6) our numerical calculation is not symmetric with respect to the inversion of the sign of  $V_{dc}$ . This difference arises from the fact that Eq. (6) is derived assuming a static  $\mathcal{F}$  and linearized  $h_{eff}$ , whereas in our calculation, we do include their complete dependence on  $\delta z$ , and therefore on  $V_{dc}$ .

To conclude, we propose a novel approach to obtain the Quantum Spin Tunneling (QST) of the Fe atom, combining LZ and LZSM. We note that LZ was used to determine QST in single-molecule magnets, where the prefactors that relate  $\delta_l$  in eq. (5) are known. In our case  $\delta_l$  depends both on  $\Delta$  and  $\alpha q v_s / z_n k$ . Importantly, the resonance pattern of the LZSM permits one to infer  $\alpha q v_s / z_n k$ . Combining both LZ and LZSM it should be possible to determine the quantum spin tunneling splitting  $\Delta$ . It is important to note that LZ protocol is not efficient to carry out control over the spin magnetization because it requires a very small sweeping rate and therefore operation times much longer than those of LZSM (see SM for details).

In summary, we have proposed an approach to control the spin of individual magnetic adatoms using ESR-STM instrumentation that, unlike previous work, operates non-resonant pulses, leveraging both on LZ and LZSM mechanisms associated to avoided crossings in the

spectrum. Specifically, we have studied in detail the paradigmatic case of Fe on MgO<sup>19</sup>. Whereas the time scale for control is in the same range that Rabi flipping times, our approach entails significantly smaller *RF* frequencies. In addition, by combining LZ and LZSM we have shown that it is possible to determine the magnitude of the quantum spin tunneling splitting  $\Delta$ .

We thank Philip Willke, Andreas Heinrich and María José Sánchez for useful discussions. A.F. acknowledges

ANPCyT (PICT2019-0654). A.F., S.S.G. and S.A.R. acknowledge CONICET (PUE22920170100089CO and PIP11220200100170) and partial financial support from UNNE. J.F.R. acknowledges financial support from FCT (Grant No. PTDC/FIS-MAC/2045/2021), SNF Siner-gia (Grant Pimag, CRSII5\_205987), Generalitat Valen-ciana funding Prometeo2021/017 and MFA/2022/045, and funding from MICIIN-Spain (Grant No. PID2019-109539GB-C41).

---

<sup>1</sup> A. Abragam and B. Bleaney, *Electron Paramagnetic Resonance of Transition Ions* (Oxford University Press, Oxford, 1970).

<sup>2</sup> L. M. Vandersypen and I. L. Chuang, *Reviews of modern physics* **76**, 1037 (2005).

<sup>3</sup> S. Haroche and J.-M. Raimond, *Exploring the quantum: atoms, cavities, and photons* (Oxford university press, 2006).

<sup>4</sup> R. Hanson and D. D. Awschalom, *Nature* **453**, 1043 (2008).

<sup>5</sup> V. Ivakhnenko, S. N. Shevchenko, and F. Nori, *Physics Reports* **995**, 1 (2023).

<sup>6</sup> S. N. Shevchenko, S. Ashhab, and F. Nori, *Physics Reports* **492**, 1 (2010).

<sup>7</sup> W. D. Oliver and S. O. Valenzuela, *Quantum Information Processing* **8**, 261 (2009).

<sup>8</sup> M. J. Everitt, P. Stiffell, T. Clark, A. Vourdas, J. Ralph, H. Prance, and R. Prance, *Physical Review B* **63**, 144530 (2001).

<sup>9</sup> J.-Q. You and F. Nori, *Nature* **474**, 589 (2011).

<sup>10</sup> X. Tan, D.-W. Zhang, Z. Zhang, Y. Yu, S. Han, and S.-L. Zhu, *Physical Review Letters* **112**, 027001 (2014).

<sup>11</sup> W. Wernsdorfer and R. Sessoli, *science* **284**, 133 (1999).

<sup>12</sup> W. Wernsdorfer, R. Sessoli, A. Caneschi, D. Gatteschi, and A. Cornia, *Europhysics Letters* **50**, 552 (2000).

<sup>13</sup> G. Cao, H.-O. Li, T. Tu, L. Wang, C. Zhou, M. Xiao, G.-C. Guo, H.-W. Jiang, and G.-P. Guo, *Nature Communications* **4**, 1401 (2013).

<sup>14</sup> E. Dupont-Ferrier, B. Roche, B. Voisin, X. Jehl, R. Wacquez, M. Vinet, M. Sanquer, and S. De Franceschi, *Physical review letters* **110**, 136802 (2013).

<sup>15</sup> G. Fuchs, G. Burkard, P. Klimov, and D. Awschalom, *Nature Physics* **7**, 789 (2011).

<sup>16</sup> A. Ferrón, D. Domínguez, and M. J. Sánchez, *Physical Review B* **82**, 134522 (2010).

<sup>17</sup> P. R. Forrester, F. Patthey, E. Fernandes, D. P. Sblendorio, H. Brune, and F. D. Natterer, *Physical Review B* **100**, 180405 (2019).

<sup>18</sup> J. Hwang, D. Krylov, R. Elbertse, S. Yoon, T. Ahn, J. Oh, L. Fang, W.-j. Jang, F. H. Cho, A. J. Heinrich, et al., *Review of Scientific Instruments* **93** (2022).

<sup>19</sup> S. Baumann, W. Paul, T. Choi, C. P. Lutz, A. Ardavan, and A. J. Heinrich, *Science* **350**, 417 (2015).

<sup>20</sup> J. L. Lado, A. Ferrón, and J. Fernández-Rossier, *Physical Review B* **96**, 205420 (2017).

<sup>21</sup> P. Willke, T. Bilgeri, X. Zhang, Y. Wang, C. Wolf, H. Aubin, A. Heinrich, and T. Choi, *ACS nano* **15**, 17959 (2021).

<sup>22</sup> Y. Wang, M. Haze, H. T. Bui, W.-h. Soe, H. Aubin, A. Ardavan, A. J. Heinrich, and S.-h. Phark, *npj Quantum Information* **9**, 48 (2023).

<sup>23</sup> Y. Wang, Y. Chen, H. T. Bui, C. Wolf, M. Haze, C. Mier, J. Kim, D.-J. Choi, C. P. Lutz, Y. Bae, et al., *Science* **382**, 87 (2023).

<sup>24</sup> P. Willke, W. Paul, F. D. Natterer, K. Yang, Y. Bae, T. Choi, J. Fernández-Rossier, A. J. Heinrich, and C. P. Lutz, *Science advances* **4**, eaao1543 (2018).

<sup>25</sup> P. Willke, Y. Bae, K. Yang, J. L. Lado, A. Ferrón, T. Choi, A. Ardavan, J. Fernández-Rossier, A. J. Heinrich, and C. P. Lutz, *Science* **362**, 336 (2018).

<sup>26</sup> P. Willke, K. Yang, Y. Bae, A. J. Heinrich, and C. P. Lutz, *Nature Physics* **15**, 1005 (2019).

<sup>27</sup> P. Willke, A. Singha, X. Zhang, T. Esat, C. P. Lutz, A. J. Heinrich, and T. Choi, *Nano Letters* **19**, 8201 (2019).

<sup>28</sup> K. Yang, Y. Bae, W. Paul, F. D. Natterer, P. Willke, J. L. Lado, A. Ferrón, T. Choi, J. Fernández-Rossier, A. J. Heinrich, et al., *Physical review letters* **119**, 227206 (2017).

<sup>29</sup> T. S. Seifert, S. Kovarik, C. Nistor, L. Persichetti, S. Stepanow, and P. Gambardella, *Physical Review Research* **2**, 013032 (2020).

<sup>30</sup> T. S. Seifert, S. Kovarik, P. Gambardella, and S. Stepanow, *Physical Review Research* **3**, 043185 (2021).

<sup>31</sup> T. S. Seifert, S. Kovarik, D. M. Juraschek, N. A. Spaldin, P. Gambardella, and S. Stepanow, *Science advances* **6**, eabc5511 (2020).

<sup>32</sup> J. R. Gálvez, C. Wolf, F. Delgado, and N. Lorente, *Physical Review B* **100**, 035411 (2019).

<sup>33</sup> K. Yang, W. Paul, F. D. Natterer, J. L. Lado, Y. Bae, P. Willke, T. Choi, A. Ferrón, J. Fernández-Rossier, A. J. Heinrich, et al., *Physical Review Letters* **122**, 227203 (2019).

<sup>34</sup> S. Baumann, F. Donati, S. Stepanow, S. Rusponi, W. Paul, S. Gangopadhyay, I. Rau, G. Pacchioni, L. Gragnaniello, M. Pivetta, et al., *Physical review letters* **115**, 237202 (2015).

<sup>35</sup> S. A. Rodríguez, S. S. Gómez, J. Fernández-Rossier, and A. Ferrón, *Physical Review B* **107**, 155406 (2023).

<sup>36</sup> D. Gatteschi, R. Sessoli, and J. Villain, *Molecular nanomagnets*, vol. 5 (Oxford University Press, USA, 2006).

<sup>37</sup> A. Ferrón, S. A. Rodríguez, S. S. Gómez, J. L. Lado, and J. Fernández-Rossier, *Physical Review Research* **1**, 033185 (2019).

<sup>38</sup> The small ringing oscillations of the magnetization once  $V_{rf}$  is switched off are due to are associated to the free evolution of a state linear combination of two different adiabatic states. The oscillation period is controlled by

$\sqrt{\Delta^2 + \varepsilon^2}$  (see color lines in Fig. 2 for  $t > t_{pump}$ )